Surfactant-mediated growth of Ge on Si(111)

M. Horn-von Hoegen,* M. Copel, J. C. Tsang, M. C. Reuter, and R. M. Tromp
IBM Research Division, Thomas J. Watson Research Center, P.O. Box 218, Yorktown Heights, New York 10598
(Received 30 November 1993; revised manuscript received 24 June 1994)

The introduction of a surfactant changes the growth in the Si(111)/Ge system from islanding to a continuous film. A Sb monolayer floats at the growth front without detectable incorporation in the growing film. The surfactant strongly influences the growth kinetics and prevents intermixing or indiffusion of Ge or Si. Up to 8 ML thickness the Ge film is completely strained and pseudomorphic; for thicker films the strain due to the 4.2% misfit is relieved by the generation of defects, which are finally all confined in a dislocation network at the interface. Low-defect, fully relaxed epitaxial Ge films of arbitrary thickness can be grown. Similarly, low-defect relaxed Si can be grown on Ge(111). Medium-energy ion scattering, high-resolution transmission electron microscopy, x-ray-photoelectron spectroscopy, and Raman scattering show that the crystal quality of these Ge films is excellent.

I. INTRODUCTION

The growth of thick, low-defect, lattice mismatched films of one semiconductor on another is an essential requirement for many modern device applications. Silicon-germanium heterostructures such as embedded layers and superlattices have several desirable features, which have spurred intensive research in recent years. For instance, Ge photodetectors or waveguides on a Si substrate are only possible if thick, high-quality Ge films can be grown. The folded band structure of a Si-Ge superlattice may allow direct transitions between the conduction and the valence band and therefore serve as photon emitter and detector. Heterobipolar transistor devices with a base consisting of a 10% Ge alloy yield transition frequencies comparable with GaAs devices.[1]

In general there are two problems that complicate this seemingly simple requirement. First, growth of one material on another frequently leads to islanding, due to a difference in surface free energy, a mismatch in lattice constants, or both.[2] Second, even without islanding, lattice mismatch gives rise to large strains in the overlayer, which must sooner or later be relieved by the introduction of dislocations and other crystal defects. Usually these defects thread through the entire film, limiting its usefulness for electronic applications.

Islanding can be prevented by growing with high fluxes at low temperatures. Under such conditions (the kinetic pathway) growth is dominated by kinetics, and far from equilibrium conditions. The concentration of mobile adatoms is high enough to initiate the formation of small two-dimensional (2D) islands, thereby supplying a high density of adatomic capture sites and preventing three-dimensional (3D) islanding. The temperature is just high enough to provide a moderate degree of epitaxy. Increasing the temperature, or keeping the growth rate low, or even both, results in islanding of both Ge on Si and Si on Ge. However, improved epitaxy requires growth at temperatures higher than 500 °C.

There are two reasons for islanding. First, the surface free energy differs for Si and Ge, so that Ge is able to wet a Si surface, but on a Ge surface Si immediately starts to island (Volmer-Weber growth). Adsorbing an appropriate third species (here, Sb) to terminate the surface changes the growth modes drastically.[3] The Sb acts as surfactant, lowering the energy of the solid-vacuum interface and floating at the growth front without being incorporated. The strong segregation is attributed to the surface free energies of *both* Ge and Si being much lower with a monolayer of Sb than without. Selective change of the activation energies some of the growth processes[4] causes island-free growth of both Ge on Si and Si on Ge. The reduction in mobility of the deposited atoms kinematically inhibits islanding. But due to the higher growth temperature of 600 °C, all Ge films thinner than 8 ML show excellent epitaxy (1 ML $=7.83\times10^{14}$ atoms/cm^2).

The second reason for islanding is the significant lattice mismatch of 4.2% resulting in an increase of strain energy with film thickness. This causes Ge to start islanding in form of 3D clusters on Si after 3-ML film thickness (Stranski-Krastanov growth).[2,5]

Even with a surfactant, it is not possible to compensate the buildup of strain with increasing coverage. Initially, the film quality is high, as strain is unrelaxed. At 8-ML (1 ML $=7.83\times10^{14}$ atoms/cm^2) Ge coverage, however, the film quality degrades rapidly and drastically due to the injection of defects, even though still no islanding occurs. At this stage the overgrown Si capping layers show twinning defects and poor crystal quality. Thus, although initial growth is encouraging, in particular if one is interested in fabricating short period superlattices, the 4.2% lattice mismatch between Si and Ge starts to play a role after only 8 ML of Ge. At first sight this situation looks rather hopeless for growth of thicker films. Elaborate strategies involving graded buffer layers[6,7] and even superlattices have been designed to try to keep the defect level in the top layer as low as possible. But such efforts are only fully effective for extremely thick buffer layers, and complicate the procedure for fabricating the desired structures.

In this paper we show that if Sb-mediated growth of

0163-1829/94/50(15)/10811(12)/$06.00 ©1994 The American Physical Society

Ge on Si(111), or Si on Ge(111), is continued after the defects have started to form, the defects will eventually disappear again from the film, leaving only a dislocation network at the Si/Ge interface, without any defects threading to the surface.[8,9] The resulting films are fully relaxed, and of excellent crystal quality.

These low-defect, strain-relieved epitaxial films may be suitable for device fabrication, or may serve as a template for further growth. One possibility would be the growth of GaAs on a Si substrate, with Ge as an intermediate layer. In this paper we will not pursue such possibilities, but focus instead on the growth and characterization of Ge/Si epitaxial films.

II. EXPERIMENT

All samples were grown in an ultrahigh-vacuum medium-energy ion scattering (MEIS) system coupled to a molecular-beam epitaxy (MBE) apparatus and a surface analysis system with x-ray-photoelectron spectroscopy (XPS) as well as low-energy electron diffraction (LEED) capabilities.[10,11] Samples can be transferred between chambers under vacuum. The vacuum level throughout the system is below 5×10^{-11} Torr. Samples are introduced from atmosphere through a load-lock system, and degassed at 600 °C for a few hours. After brief additional degassing at 900 °C, the sample is lightly sputtered (500-eV Ar, 10^{14} ions/cm^2) in order to remove part of the native oxide together with any surface contamination. Finally, the native oxide is flashed off at 1050 °C. At this stage the sample displays a bright and sharp (7×7) LEED pattern. No impurities are detected with either MEIS and XPS. Contamination during growth is drastically prevented by the passivation of the surface due to the Sb and not detectable.

The sample is then transferred to the MBE/XPS chamber for growth. Deposition took place at about 600 °C, unless otherwise indicated. The evaporators are located in a separate MBE chamber, which is connected to the main chamber. Small apertures between the chambers restrict the flux of evaporated material, so only the sample is exposed.

Ge is evaporated from a boron nitride Knudsen cell, Sb from a quartz Knudsen cell, and Si from an *e*-beam evaporator. Electrostatic deflection plates remove Si ions from the molecular beam, preventing ion irradiation of the growing film. All evaporators are water cooled. Typical growth rates are between 0.1 and 1 ML per minute. All evaporators were equipped with quartz microbalances to estimate the flux and film thickness.

To initiate growth, the sample is heated to the desired temperature (by direct current heating) and then exposed to the Sb flux. The Sb coverage saturates close to 1 ML. Next, the desired Ge and/or Si films are grown, either with or without a small Sb flux simultaneously impinging on the sample. We find that excellent films can be grown either way, although at slightly lower temperature without a simultaneous Sb flux. As shown later, Sb incorporation is extremely small both ways. Thin Ge films were immediately capped with a Si layer of about 20 ML thickness, also in a continuous Sb flux.

The MBE growth system is attached to an MEIS system, described in detail elsewhere.[12] The ion scattering data were obtained with a newly developed two-dimensional detector, collecting simultaneously a 20° spread of angles and a range of energy 1.85% of the pass energy.[11] We achieve an energy resolution of at least $\Delta E/E=1.25\times10^{-3}$, i.e., 250 eV for 200-keV He^+ ions. The new detector provides a higher efficiency and therefore a lower beam dose, since more ions are detected at the same time due to the wider energy range which is accepted.

Data were taken with 200-keV He^+ ions incident in the $[00\bar{1}]$ direction. Due to the high ion energy, the neutralization rate was only 25%, measured separately with a solid-state detector equipped with deflection plates. Helium ions were used to separate clearly the Sb, Ge, and Si species. The analyzer and detector were positioned near double-alignment arrangement at 54.75° scattering angle ($[11\bar{1}]$ direction). The energy spectra shown here are integrated over an angular range of typically ±1.5° about an angle of 57.3° or 48.1°, providing different mass separation and depth resolution. Due to the efficiency of the new 2D detector, ion scattering data with good statistics were obtained at a beam dose as low as 7×10^{13} ions/cm^2 to avoid significant damage of Ge films thicker than 8 ML (changes in the Ge signal for the channeling spectra were below 1%). The random spectra were obtained by an azimuthal rotation of 7.7° and a polar rotation of 4.0°, relative to the $[00\bar{1}]$ channeling spectra. Low-energy electron diffraction patterns were observed with rearview LEED optics before the MEIS measurements took place.

Finally, after inspection with the *in situ* analytical techniques, the sample is removed from the vacuum system through the load lock. Up to two samples can be prepared and analyzed per day, allowing rather extensive and systematic studies of the epitaxial growth process.

A number of samples were further analyzed with high-resolution transmission electron microscopy (HR TEM) and Raman scattering. TEM was used to determine the micromorphology and defect structure of the epitaxial films in detail. In this paper we will show some of the results obtained with this technique. Full and detailed accounts of our findings are published elsewhere.[8,9]

The phonon structure of the sample can be studied with Raman scattering, a technique well suited for the analysis of thin Ge films on Si.[13,14] Si-Si, Ge-Ge, and Si-Ge phonons are clearly separated in the energy-loss spectrum. In particular, the appearance of a clearly identifiable signal for the Si-Ge phonon is significant as it allows one to determine the degree of intermixing across the Si-Ge interface. The line shape and position of the Ge-Ge phonon contains information on the strain in the epitaxial Ge layer. When the Ge film is uniformly strained, this peak is shifted to larger loss energy, but it is sharp. Incomplete strain relaxation, accompanied by extended defect structures throughout the film, give rise to inhomogeneous strain fields, shifting the Ge-Ge phonon peak to lower loss energy and giving rise to considerable broadening of the line shape.

III. RESULTS

A. Reconstruction of Sb on Si(111) and Ge(111)

Depending on the absorption temperature, Sb forms different reconstructions on the Si(111) surface, each with a different coverage,[15] but all removing the stacking fault of the (7×7).

The Sb-($\sqrt{3}\times\sqrt{3}$)$R30°$ structure is formed by trimers of Sb atoms centered on the T_4 site of the Si lattice in a temperature range around 650 °C.[16] Each Sb atom is bonded with one electron to a Si top atom, with two electrons to the two neighboring Sb atoms. The remaining two electrons form a lone pair orbital. Sb fully passivates the Si(111) surface dangling bonds, thus reducing its chemical reactivity and changing the surface properties.[16–18] The surface free energy is lowered by the Sb, due to this energetically favored filling of dangling bonds.

The Sb-(2×1) structure consists of zigzag chains of Sb atoms sitting on the top atoms of the Si surface running $\langle 1\bar{1}0\rangle$ directions. The (2×1) structure is formed at lower temperatures than the ($\sqrt{3}\times\sqrt{3}$) but is usually apparent at defects such as step edges, domain boundaries, dislocations, etc.[19] We expect the electronic configuration of the Sb-(2×1) to be similar to the ($\sqrt{3}\times\sqrt{3}$) structure, i.e., one electron in a backbond to the Si substrate, two electrons in covalent bonds with neighboring Sb atoms in the chain, and two electrons in a lone pair orbital.

Exposing Si at 600 °C to Sb, we were able to achieve an Sb saturation coverage of about 0.9 ML. The LEED pattern shows a diffuse ($\sqrt{3}\times\sqrt{3}$) and a less intense (2×1) structure with high background. This temperature is too low to form a well-ordered ($\sqrt{3}\times\sqrt{3}$) structure over large areas, since Si atoms have to be moved in order to rearrange the original (7×7) structure into a bulklike Si structure. A much improved ($\sqrt{3}\times\sqrt{3}$) reconstruction [LEED pattern with very low background, no (2×1) intensity, and sharp spots] is obtained after growth of Si on Si(111) at 600 °C in the presence of an Sb flux, resulting in an Sb coverage of about 0.95 ML. During growth, the additional and mobile adatoms are directly arranged in the energetically more favorable ($\sqrt{3}\times\sqrt{3}$) structure.[20]

On the Ge films, grown in these experiments, the Sb forms a (2×1) structure with a coverage of 0.8–0.9 ML of Sb. Scanning tunneling microscopy (STM) measurements also show (2×1) domains on the Ge.[21] The Ge (2×1) structure consists of chains running along the $\langle 1\bar{1}0\rangle$ directions, as on Si(111).

B. Ge on Si and Si on Ge

Figure 1(a) shows the backscattered ion yield as a function of energy after the deposition of 3-ML Ge at 600 °C both for channeling and random incidence geometry. With the ion beam incident in the [00$\bar{1}$] channeling direction, subsurface atoms in bulk lattice sites are shadowed by the surface atoms and do not contribute to the spectra. Therefore this geometry is used to determine the crystal quality. The spectra taken in random incidence geometry, however, show all atoms of the crystal. Due to electronic energy losses of the ions traversing the crystal,

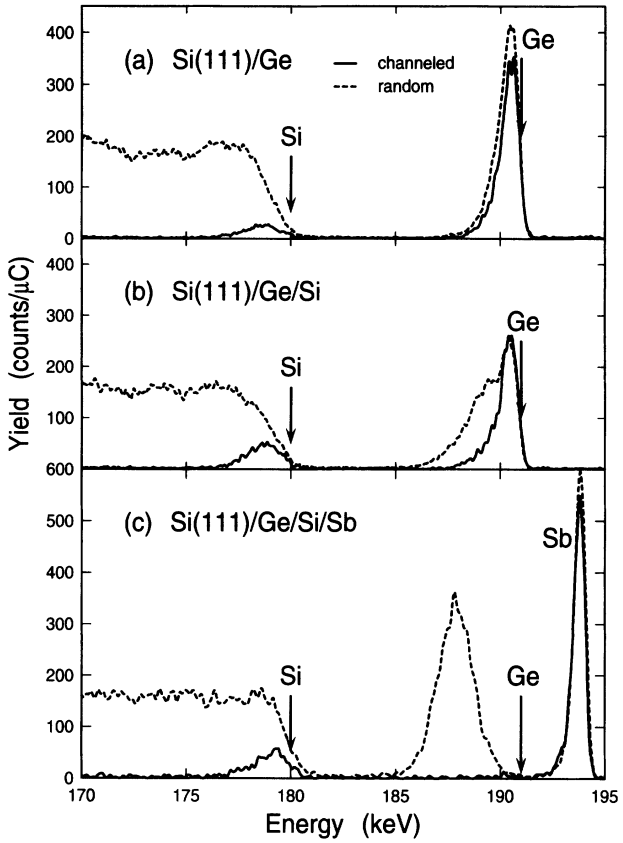

FIG. 1. Ion backscattering spectra for 3-ML Ge films with and without a Si cap. Both random and channeling spectra are shown. (a) Initial nonislanding Ge overlayer without any Si cap. (b) Ge film after deposition of 6 ML of Si without a Sb passivation layer. Large amounts of the Ge are still apparent at the surface due to immediate islanding of the Si (Volmer-Weber growth). The tail on the Ge peak in the randomly incident spectrum is due to Ge buried by Si islands. (c) A 4.5-ML Ge film grown with Sb codeposition and covered by a 20-ML Si film. No islanding of the Si is visible. The Ge is totally covered with Si, as seen by the shift to lower energies.

ions scattered from deeper atoms appear at lower energies in the spectra. The different species are separated by the kinematic loss factor for elastic scattering, with higher masses appearing at higher energy. Thus, spectra obtained in the random geometry reflect the composition and depth structure of the sample. An overview of the technique of medium-energy ion scattering is given in Ref. 10. The compact shape of the Ge peak in Fig. 1(a), and the absence of a tail at the low-energy side of this peak, indicate that this 3-ML-thick Ge film is continuous and flat.

First, let us examine how Si will nucleate on the 3-ML Ge film. Later, we will discuss growth of thicker Ge films. When we evaporate 6 ML of Si on top of a 3-ML Ge film, the spectra seen in Fig. 1(b) are obtained. Part of the Ge is still on top of the surface, as seen in the unshifted Ge surface peak. The shoulder in the random incident spectrum is caused by Si islanding on top of the Ge film, without wetting the entire surface (Volmer-Weber growth). The ions undergo inelastic energy losses

in the Si islands before and after scattering in the Ge film, shifting that part of the Ge signal and causing the shoulder. The arrows in this and other spectra point to the expected surface peak positions for the indicated species.

Growth of Si on the Sb terminated surface results in quite different behavior, as seen in the spectra of Fig. 1(c). The Ge peak is shifted to lower energies de to the energy losses in the 20-ML-thick Si capping layer. The compact Gaussian shape reflects the absence of islands in both the Ge layer and the Si cap. The epitaxial nature of the heterolayers is seen in the very low minimum yield. This quantity is defined as the ratio of backscattering signal in channeling geometry, divided by that in random geometry. χ_{min} is lower when the crystal quality is better.

Without a surfactant, continuous Ge films could only be grown up to 3 ML thick, as shown above, the so-called Stranski-Krastanov layer. The extensive islanding of 10-ML Ge on Si(111), with an average island height of about 80 Å, is apparent in the long, low-energy tail of the Ge peak in the random incident spectrum in Fig. 2(a). The Ge surface peak shows the Stranski-Krastanov layer of about 3 ML. The high minimum yield of $\simeq 10\%$ below the surface peak of the Ge is caused by defects and dislocations relieving the strain built up by the lattice mismatch of 4.2%. The LEED pattern shows the well-known (5×5) reconstruction of this system [Fig. 3(a)].[22–25] The high background intensity for higher electron energies (91 eV) is caused by roughness of the surface and a high number of defects and dislocations.

Again, codeposition of Sb drastically changes the

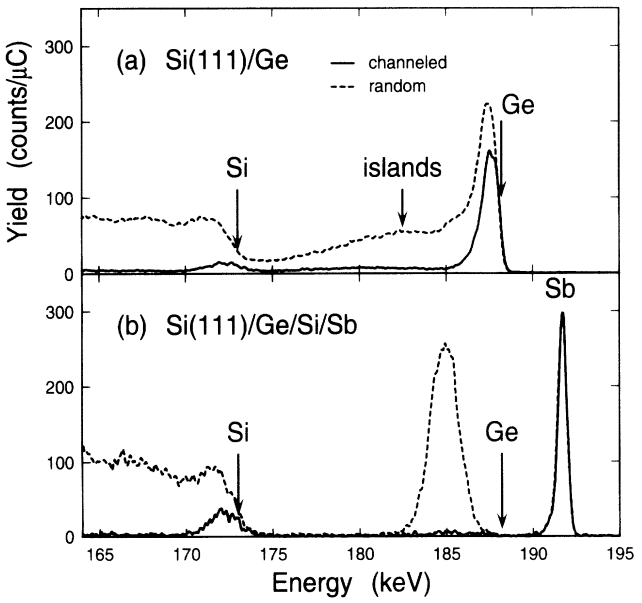

FIG. 2. Ion backscattering spectra for Ge/Si(111) films grown at 600 °C. Both random and channeling spectra are shown. (a) Deposition of 10-ML Ge at 600 °C results in Ge islands on a 3-ML-thick Stanski-Krastanov layer of Ge. (b) A 7-ML Ge film grown at 600 °C with the surfactant Sb and capped with 20 ML of Si show no sign of islanding. The low yield in the channeling spectrum reflects the excellent crystalline quality of the Ge film.

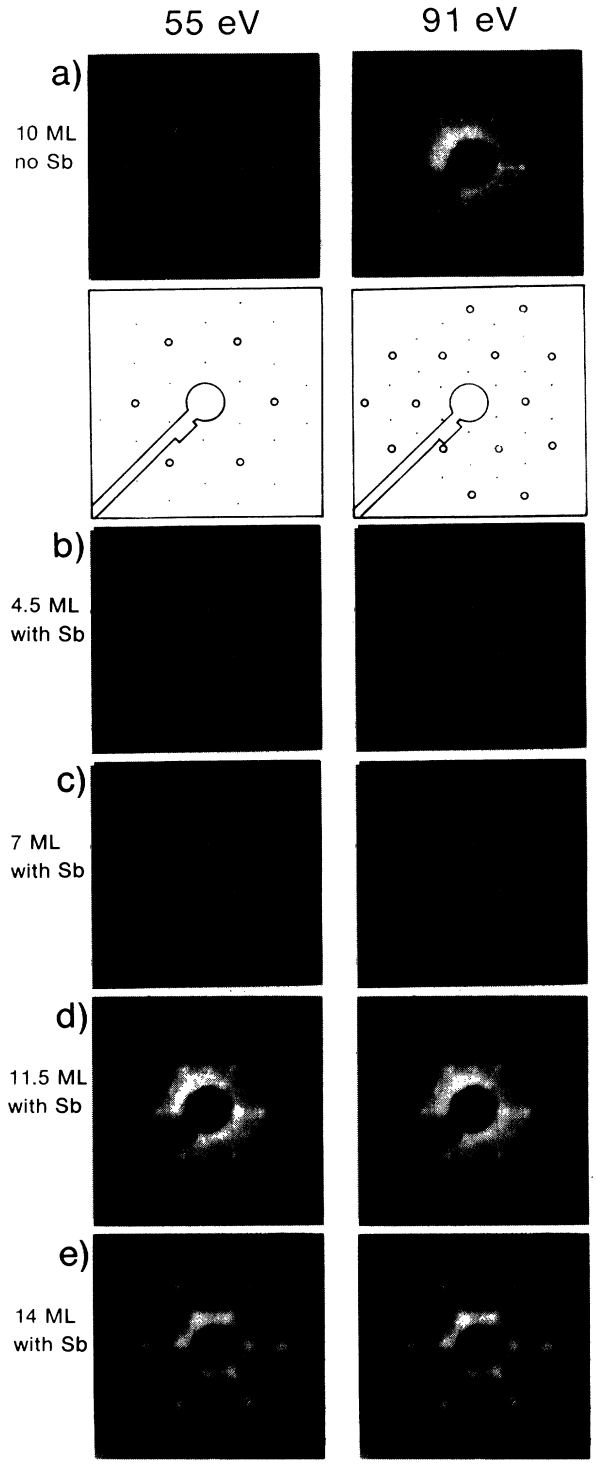

FIG. 3. LEED pattern of the films grown at 600 °C for electron energies of 55 and 91 eV. The inset shows the position of the integral order spots (circles) and the position of the $(\sqrt{3}\times\sqrt{3})$ spots (points). (a) 10 ML of Ge without surfactant results in a (5×5) reconstruction. (b)–(d) Different amounts of Ge covered with 20-ML Si grown with Sb as surfactant. The LEED pattern changes from a brilliant $(\sqrt{3}\times\sqrt{3})$ reconstruction with low background (4.5-ML Ge) to a mixture of diffuse (2×1) and $(\sqrt{3}\times\sqrt{3})$ reconstruction with high background (14-ML Ge), indicating increasing defect densities.

growth mode from Stranski-Krastanov to island-free growth. A Ge film of 7 ML thickness no longer islands but wets the entire Si surface, as seen in the compact, Gaussian shape of the Ge peak at random incidence [Fig. 2(b)]. The Ge film was capped with a 20-ML-thick Si film, to achieve shadowing of Ge atoms on lattice sites. Therefore, the channeling spectrum provides a sensitive test of epitaxy, i.e., deviation of atoms from lattice positions. The low minimum yield (as defined above) of about 2.5% (1.2% for double alignment) is similar to $\chi_{\min}$ for bulk Ge.

For this film the LEED pattern at 55 eV shows sharp integer order spots and a brilliant $(\sqrt{3}\times\sqrt{3})R30°$ structure [Fig. 3(b)]. This, and the absence of facet spots, reflects a flat surface of the Si capping layer with terraces and $(\sqrt{3}\times\sqrt{3})$ domains wider than 100 Å. Although at this energy a (2×1) superstructure would give rise to very intense fractional order reflections, only very faint (2×1) intensity is visible, indicating a highly perfect surface.[19] The higher energy of 91 eV is more sensitive to defects and disorder due to the large scattering vector, but still shows a very brilliant $(\sqrt{3}\times\sqrt{3})$ structure with low background.

Surprisingly, the LEED pattern taken direct after the growth of 7 ML of Ge without the Si capping layer shows very broad spots with high background, indicating a rough surface with terrace widths in the order of five to ten atoms. STM measurements[21] also show in this initial stage of growth a surface roughness of typical 1–3-bilayer height and terrace widths as seen with LEED. Such a rough growth stage, with the surface composed of microfacets of (113) type with a size of about 60–100 Å, has also been recently observed in a high-random LEED study.[26] Transmission electron microscopy inspection of this film shows no defects or dislocations in the grown Ge and Si layers.

This Ge film must be pseudomorphic, since we do not observe dislocations or defects. Part of the strain is relieved by tetragonal distortion of the Ge lattice, which results in a distortion of the unit cell and shifts the angular position of the blocking minima in the Ge film. This is seen in Fig. 4 for a 6-ML-thick embedded Ge film where the blocking minimum of the Ge signal at 54.75° is shifted by about 0.3° to larger scattering angles with respect to the minimum in the Si bulk. All other minima are also shifted by about the same amount. Due to the thin Ge film thickness, the shift of the blocking minimum is not as large as seen by Mantl, Kasper, and Jorke[27] for a thick layer. While tetragonal distortion of the Ge lattice is clearly present in these films, surface roughness may allow partial relaxation of the Ge film towards the bulk Ge lattice constant.[26]

C. Embedded films

In Fig. 5 we show spectra for embedded Ge films grown with an Sb termination as a function of Ge film thickness. The Ge films do not island even for a thickness of 14 ML and are uniformly covered by the Si capping layer as seen in the compact shape of the Ge peak, which is shifted to lower energies. The depth location of

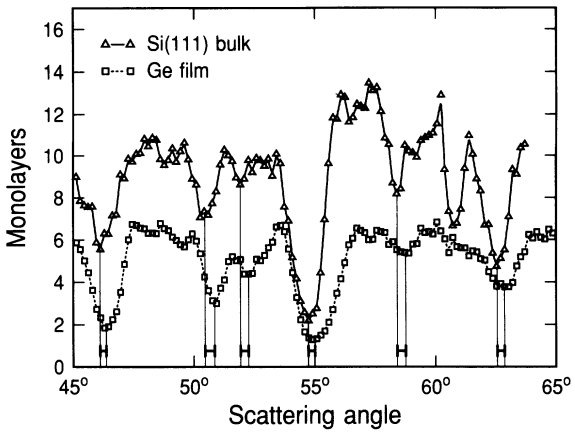

FIG. 4. Angular distribution of ion backscattering intensity for an embedded 6-ML-thick Ge film: Solid line, Si(111) bulk spectrum. Dashed line, strained Ge film; the blocking minima are shifted by 0.3° towards higher scattering angles, reflecting the change in bond length in the strained Ge film. The thin vertical lines indicate the position of the blocking minima.

the Ge is apparent from the dip in the Si random spectrum, which gets deeper with increasing Ge film thickness. But the crystal quality of the heterolayers diminishes drastically for Ge films thicker than 8 ML. As the Ge coverage increases, a larger portion of the Ge is visible in the channeling spectra (Fig. 5), indicating Ge on nonlattice sites.

The minimum yield $\chi_{\min}$, plotted in Fig. 6, is close to its perfect crystal value up to a thickness of 8 ML, and increases rapidly at higher coverages up to more than 20% for a 15-ML Ge film (single alignment). Below 8 ML, the Ge film is pseudomorphic with the Si substrate, adjusting to the smaller substrate lattice constant with a tetragonal distortion of the Ge lattice. Above 8 ML, the strain energy becomes too large and drives the introduction of strain-relieving defects. As a result, the crystal quality of both the embedded Ge film and the Si capping layer deteriorate, giving rise to the increase in $\chi_{\min}$. The values for $\chi_{\min}$, however, remain still much lower than those reported for growth without Sb.[28]

TEM inspection[9] of the 14-ML Ge film shows the formation of dislocations and defects in the Ge and Si. These dislocations appear after the deposition of more than 8-ML Ge, as seen in the sharp increase of the minimum yield (Fig. 6). The driving force for the formation of dislocations is the strain, which now is relieved, shifting the lattice constant toward the value of bulk Ge.

The quality of the Si capping layer is also diminished, as seen in the increased yield of the Si surface peak in channeling geometry (reflecting the visible Si atoms of the capping layer). This is also confirmed with TEM measurements, showing twinning of the Si capping layer for Ge films thicker than 8 ML. We observed twinning in the Si overlayer, even though defects or dislocations in the underlying Ge film could not be identified in cross-sectional TEM samples. A large portion of the ions are already dechanneled in the Si capping film, seen as an increased Si yield in channeling geometry [Figs. 5(c) and

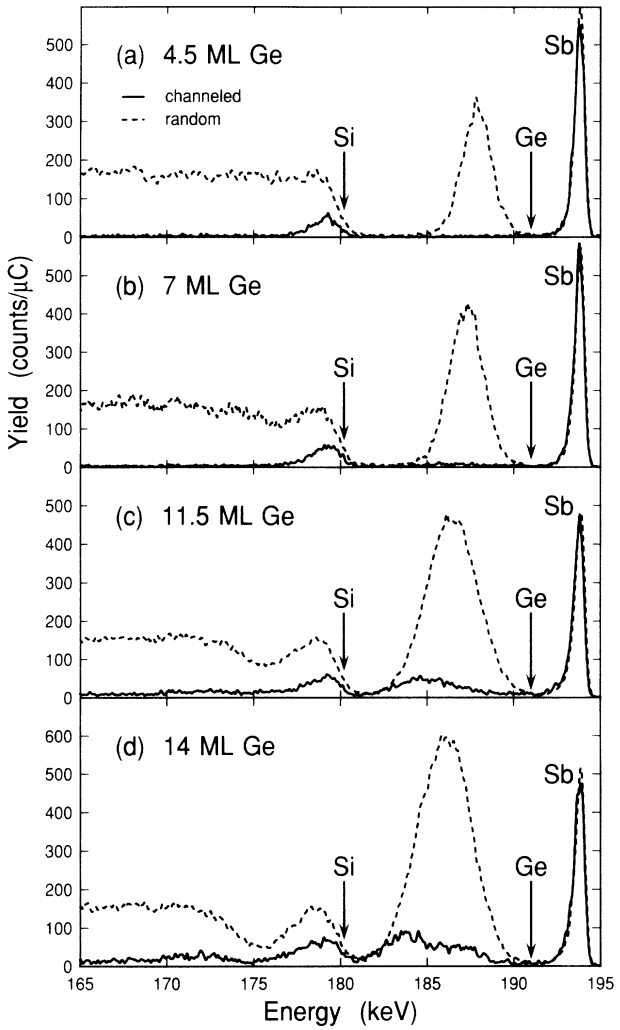

FIG. 5. Ion backscattering spectra for Ge films of different coverages embedded in Si grown at 600 °C. Both random and channeling spectra are shown. The yield for channeling geometry increases for Ge film thickness exceeding 8 ML, indicating diminishing crystalline quality. The dip in the randomly incident spectrum of the Si signal reflects the depth location of the embedded Ge films. The arrows mark the surface peak position of the different species.

5(d)]. This dechanneling of the ion beam additionally increases the minimum yield of the Ge film.

The LEED pattern of the Si capping layer deteriorates with increasing Ge film thickness [Figs. 3(b)–3(d)]. The pattern changes from a brilliant $(\sqrt{3}\times\sqrt{3})$ structure with very low background and sharp spots to a mixture of very diffuse (2×1) and $(\sqrt{3}\times\sqrt{3})$ structure with high background and broadened spots. The intensity of the (2×1) spots increases with thicker Ge films, suggesting the existence of more and more defects at the surface,[19] giving rise to the simultaneous occurrence of different surface reconstructions.

The Sb-mediated growth only works properly in a narrow temperature window. Lowering the temperature below 550 °C results in poorer epitaxy of the Ge film: The random spectrum lacks structural features such as

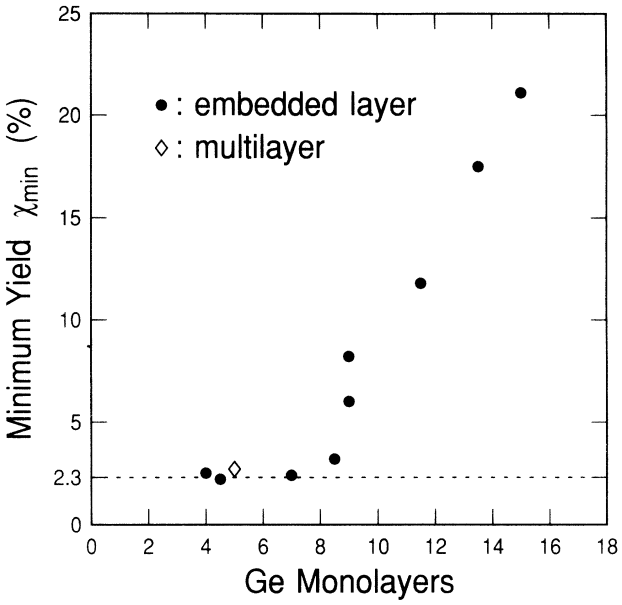

FIG. 6. Minimum yield (χ_{min}) in single-alignment geometry for embedded Ge films grown at 600 °C for different coverages. The crystalline quality drops steeply for coverages exceeding ≃8-ML Ge, where dislocations form to relieve strain.

blocking minima and the channeling spectra show an increased yield, due to Ge atoms on nonlattice sites. Increased incorporation of Sb (Ref. 20) as well as the reduced mobility of the deposited atoms cause defects.

For higher temperatures the crystalline quality is excellent, as indicated by the presence of well-developed blocking minima. But above 650 °C, strong Si-Ge intermixing and, for temperatures above 680 °C, islanding of the Ge film occurs again. Desorption of the Sb below a critical coverage of ~0.5 ML results in a growth as observed without surfactant.

D. Multilayers

The wetting of both Si with Ge and Ge with Si allows growth of superlattices with alternating Si and Ge layers. Following the same procedure as for the embedded films, a

$$\mathrm{Si(111)/Ge_5/Si_{10}/Ge_5/Si_{15}/Sb}$$

multilayer structure was grown (the index gives the number of ML).

Figure 7(a) shows a two-dimensional plot of backscattered ion intensity (see the color scale on the bottom) in random incidence geometry as function of energy (y axis) and angle (x axis), with an energy range from 200 down to 117 keV and a range of scattering angles from 30° to 110°. The Sb, Ge, and Si peaks disperse to lower energies with increasing scattering angle due to the decrease in the kinematic energy loss factor with increasing scattering angle. The Ge double peak, which is due to the two separate Ge films, is shifted to lower energies by the Si capping layer. The double Ge peak bends to lower energies at smaller scattering angles due to the thickness of

the Si capping layer, since the detected ions leave the surface under a more glancing angle and lose more energy. Therefore, the depth sensitivity is enlarged for small scattering angles, as seen in the increased width and separation of the Ge peaks. The depth structure can also be seen clearly in the dips below the Si surface peak caused by the two Ge layers. The cutoff of the spectrum at an angle of 31.3° is caused by the surface with the ions leaving under grazing angle. The superior energy resolution of the new 2D detector is seen in the very narrow Sb peak, scattered from the Sb on top of the surface. The underlying multilayer structure exhibits clear blocking

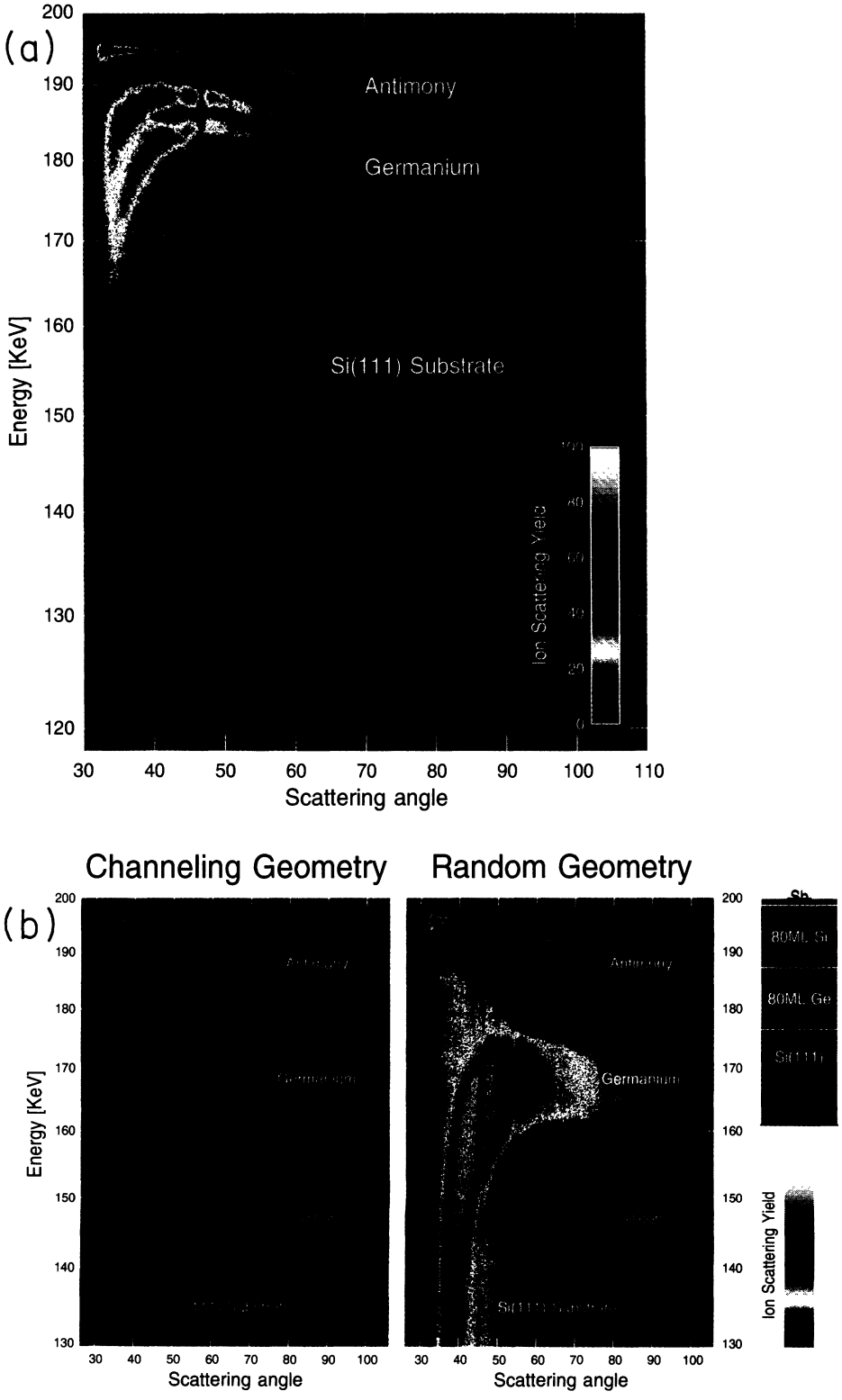

FIG. 7. Ion backscatter spectra for different Ge/Si layered structures are shown. He^+ ions with 200 keV have been used. The yield is plotted using the color look-up table shown in the inset. The ion backscatter yield is plotted both as a function of the scattering angle (x axis) and of the backscattered ion energy (y axis). (a) A $Si(111)/Ge_5/Si_{10}/Ge_5/Si_{15}/Sb$ layered structure (the subscripts indicate the thickness of the particular layer in ML) grown at 600 °C. The depth location of the two Ge layers is apparent in the weak dips in the Si signal. (b) A relaxed 80-ML Si film grown on top of a 80-ML Ge film on Si(111). Both random and channeling spectra are shown. The Ge has been deposited at 600 °C substrate temperature which has been raised up to 700 °C for the growth of the Si layer. The Sb adlayer is the topmost fine sharp line. The blocking minima are seen as vertical lines with lower intensity. The embedded Ge film is seen as an intense broadband. In the channeling spectra the location of the strain-relieving dislocations is clearly seen in the increased yield at the borders of the Ge signal.

minima in both the Si and Ge layers.

In Fig. 8 the energy spectrum of the

$$Si(111)/Ge_5/Si_{10}/Ge_5/Si_{15}/Sb$$

layered structure is shown for two different angles. The two Ge peaks can be distinguished very well in the random spectra. The spectrum taken at a scattering angle of 57.3° [Fig. 8(a)] shows a very good separation of the different species; the low yield between the peaks reflects the very low incorporation or interdiffusion rate. In the spectrum with 48.1° scattering angle [Fig. 8(b)], the Si and Ge peaks overlap a little bit, but the location of the embedded Ge layers becomes apparent in the two dips of the Si signal. The channeling spectra show a low yield, with a χ_{min} similar to the thin embedded Ge films (open rhomb. in Fig. 6). A sharp $(\sqrt{3}\times\sqrt{3})$ LEED pattern with low background also reflects very good epitaxial quality. Though the *total* Ge coverage exceeds 8 ML, no dislocations have been generated due to the intermediate Si layers, which partition the strain of the Ge films.

E. Ge-Si interdiffusion and Sb incorporation

A strong tendency to surface segregate is an important condition for the effectiveness of Sb as a surfactant. Also, for technological applications the incorporation of the Sb and interdiffusion of Si and Ge are important points. For example, the performance of a quantum well structure may be greatly enhanced if it is grown with an Sb-terminated surface.[29,30] As seen in Fig. 1(c), hardly any ion yield is detected at the Ge surface peak position. Thus a Ge concentration less than 1% was detected in the Si capping layer caused by diffusion further than 5 ML into the Si. This value is much lower than found in films grown without a surfactant on Si(100).[14] Evidently, the Sb layer on the surface reduces out diffusion of Ge into the Si overlayer. Such diffusion and intermixing is surface mediated and is strongly hindered by the Sb surface layer. As soon as a Ge or Si atom has occupied a lattice site, it is bonded in that subsurfactant position, resulting in a strongly reduced surface mobility.

The incorporation of Sb into the Ge or Si epilayer is estimated from the ion scattering data to be less than 2.5×10^{19} atoms/cm^3. This is an upper limit; the intensity in the relevant energy window could be affected by multiple scattering, too, which would cause additional intensity which may be misinterpreted as incorporated Sb. We found values which are close to the solid solubility limit of about 2×10^{19} atoms/cm^3 of Sb in bulk Si. Metzger and Allen got similar limits for Sb incorporation during Si growth accompanied by a high Sb flux at low temperatures.[31] Recent secondary ion mass spectroscopy (SIMS) results[5] give an upper limit for the incorporation of Sb into the Ge film of less than 5×10^{18} atoms/cm^3. Nakagawa, Miyao, and Shiraki have already shown that for temperatures above 400 °C, Sb is not incorporated but floats on the growing Si surface.[32,33] Even lower dopant concentrations can be achieved by choosing species with greater segregation coefficients, such as Bi.[34]

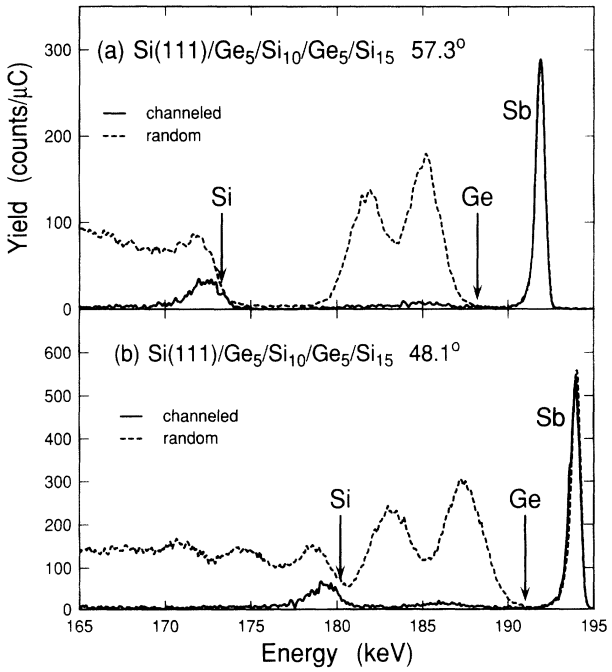

FIG. 8. Ion backscattering spectra for the $Si(111)/Ge_5/Si_{10}/G_5/Si_{15}/Sb$ layered structure (superlattice). Both random and channeling spectra are shown. (a) At a scattering angle of 57.3°, the double peaks for the two Ge layers are clearly visible in the randomly incident spectrum. (b) At the smaller scattering angle of 48.1°, the depth resolution is increased. The two small dips in the Si spectrum show the depth location of the two Ge films.

F. Strain-relieved Ge films

Several previous studies have been devoted to the structure of strain-relief defects for Sb-mediated Ge/Si(111) epitaxy.[8,9] Strain relief is accomplished with an interfacial network of Shockley partial dislocations (SPD's), characterized by alternating areas of faulted and unfaulted stacking at the Si-Ge interface. The SPD's are injected into the Ge films at thicknesses exceeding 8 ML, giving rise to a sharp increase in χ_{min} at that coverage. Once the network of SPD's is complete, the film is fully strain relieved, and regions of the film away from the interface are highly crystalline. Thus, while the bulk of the epilayer lends itself to ion channeling, there is substantial dechanneling at the interface due to the dislocations.

The effects described above are not limited exclusively to Ge growth on Si(111). In Fig. 7(b) ion backscatter spectra are shown for a Sb surfactant grown 80-ML Si film on top of an 80-ML Ge film on Si(111). Both random and channeling spectra are shown. The yield is plotted using a logarithmic color look-up table as a function of the scattering angle (x axis) and backscattered ion energy (y axis). The Sb adlayer appears in both scattering geometries as the topmost sharp thin line, explicitly displaying the kinematic loss factor depending on the backscatter angle.[10] The surface peak of the top Si is a sharp line in the channeling spectrum or a sharp edge in the random spectrum. The low yield in the channeling

spectra again shows the perfect crystal quality. The strain-relieving defects are observed in the channeling spectra as increased yield at the low- and high-energy edge of the Ge signal; at both interfaces the dislocations are confined to the interface. The strong bending of the Ge signal towards lower energies at lower angles is caused by the increasing depth sensitivity due to the more grazing exit angle (the ions lose more and more energy in the Si cap). In the random spectrum the location of the Ge layer is clearly seen in the broad dark band located in the Si signal. Both layers are strain relieved as seen in the identical position of the pronounced blocking minima.

For an embedded, strain-relieved Ge film in Si(111), there is a symmetry between the top and bottom interfaces, and the defect microstructure for the two interfaces are quite similar. By looking at a cut through Fig. 7(b), integrated over a 5° range of scattering angles centered at 89°, we can observe the size of the dechanneling peaks due to the top and bottom interfaces (Fig. 9). (We show a larger scattering angle than in previously figures; this is necessitated by the film thickness. As a consequence, there ions undergo a greater kinematic energy loss and peaks appear at lower energies than in previous spectra.) Not only do the two interfaces share a common type of defect, but the interfaces must be quite similar in structure over large regions of the samples.

Compared to growing a single strain-relieved heterolayer, it is difficult to fabricate strain-relieved multilayer structures: Because Si is less mobile than Ge, we need higher growth temperatures to get a fully evolved defect structure. The Si layer in Fig. 9 was grown at 700 °C, where there is significant Sb desorption. Therefore the Sb flux must be increased to compensate. Growth at even higher temperatures would improve the Si-layer quality. Unfortunately, this is not possible because the layer structure is only stable up to 720 °C.

G. Raman scattering

The crystal quality of the Ge film was studied by Raman scattering, which is a sensitive probe for Si-Ge intermixing and for homogeneous as well as inhomogeneous stresses in the Ge lattice. A strong and narrow Ge-Ge peak is observed at an energy characteristic of unstrained Ge (Fig. 10). The line shape is highly symmetric, evidence for the absence of inhomogeneous strains. The measured peak width of 3 cm^{-1} is consistent with low-defect Ge with a dopant concentration of 3×10^{19} Sb/cm^3, close to the solid solubility of Sb in Ge. This dopant concentration is close to the upper limit determined from the ion scattering spectra. No Si-Ge signal is found, indicating that alloying is absent in this film, in agreement with MEIS results.

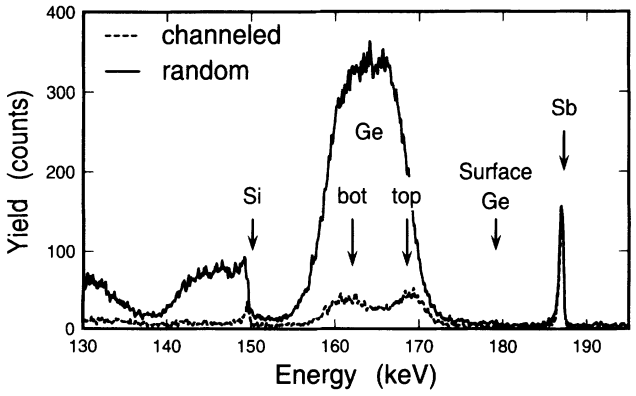

FIG. 9. Ion scattering spectrum for a thick Ge film embedded in a Si substrate. Interface defects are visible for both the Ge substrate and the Ge capping layer interfaces.

H. X-ray photoelectron spectroscopy

XPS was used to determine the efficiency with which Sb floats to the surface during growth. A set of spectra, obtained with Al $K\alpha$ radiation is shown in Fig. 11. The electron energy range shown here, from 100 to 625 eV, contains the Ge($2p$) and Sb($3p$) core levels. On the clean Si(111)-(7×7) surface, neither Ge nor Sb signals are observed. Upon adsorption of Sb, to form the $(\sqrt{3}\times\sqrt{3})$ superstructure near 1-ML Sb coverage, a clear Sb($3p$) signal appears. During initial Ge growth (up to 60-ML Ge) a small Sb flux was supplied to avoid depletion of the surface Sb. The Sb signal intensity remains constant; a steady growth in Ge signal intensity is observed. Next, the Sb flux was turned off, and Ge growth was continued to follow segregation (or incorporation) of Sb in the grow-

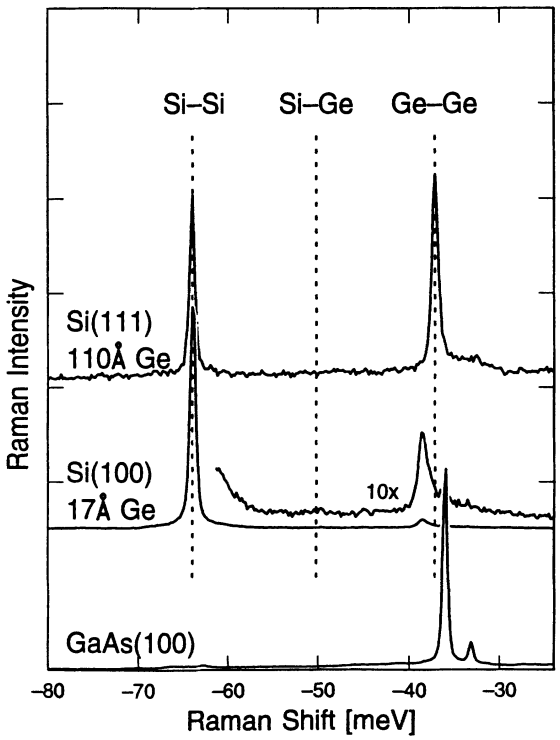

FIG. 10. Raman scattering spectrum of various Ge films grown on Si(111). For comparison, a GaAS(100) spectrum is also plotted. The unshifted position of the Ge-Ge vibrational mode indicates a strain-relieved film.

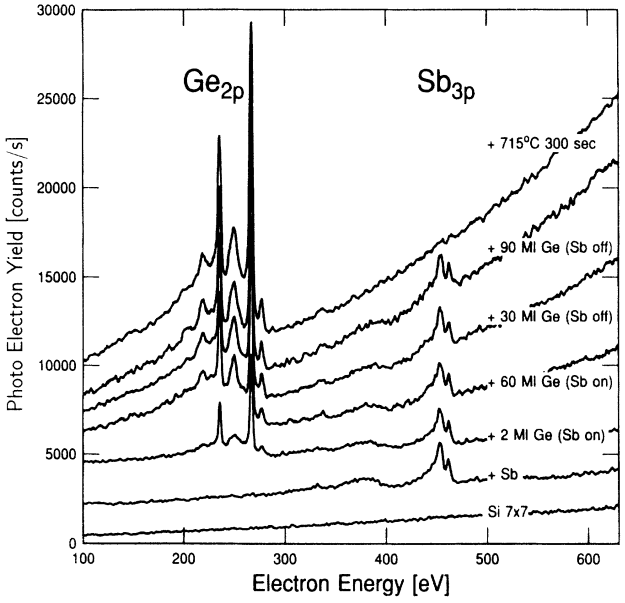

FIG. 11. X-ray photoelectron spectra for Sb/Ge/Si(111). The amplitude of the Sb signal is independent of Ge film thickness, indicating that very little of the Sb is incorporated in the Ge but floats on top of the growing Ge film. No significant desorption occurs at growth temperature.

ing film. After growth of an additional 120 ML of Ge, there is no noticeable depletion of the Sb signal. Thus, the Sb segregates to the surface with high efficiency. From these data we estimate that no more than 5×10^{19} Sb/cm^3 is incorporated into the growing Ge film. Flashing the sample to 715 °C for 5 min removes the surface Sb. Unfortunately, the Ge film is now rough, as can easily be established by visual inspection.

IV. DISCUSSION AND CONCLUSIONS

A. Growth mechanism

Any attempt at explaining the growth mechanism and observed phenomena under thermodynamic equilibrium has to take in account two important parameters: the difference in lattice constant and the surface free energy. The latter determines the possibility of wetting a substrate of element A with an epitaxial film of element B. The inequality

$$\sigma_A > \sigma_B + \sigma_i ,$$

with the free energy of the substrate surface (σ_A), the interface free energy (σ_i), and the surface free energy of the heteroepitaxial layer (σ_B), sets the condition for the epitaxial film B to wet the substrate A. In this case layer-by-layer growth (Frank–Van der Merwe) may occur, changing into the Stranski-Krastanov mode if the overlayer strain is unfavorable. If the inequality has the opposite sign, usually Volmer-Weber growth occurs, i.e., immediate islanding of the overlayer.

For heteroepitaxy one of the species, A or B, must have a lower surface free energy. Thus, if A wets B, B will in general not wet A. Any attempt at growing an $\ldots A/B/A/B\ldots$ structure has to overcome this fundamental problem. For the case of Si and Ge, Ge grows on Si(111) in a Stranski-Krastanov mode, and Si on Ge(111) in a Volmer-Weber mode. This results from the above inequality, where Ge has a lower surface free energy than Si. If the balance of surface free energies is shifted, with no other effects, an $\ldots A/B/A/B\ldots$ structure will still be difficult to achieve, since we can only switch which constituent will island.

The inequality describes the situation in thermodynamic equilibrium. By limiting kinetics, one may be able to grow a continuous film B on a substrate A, even if this is thermodynamically unfavorable. However, growth at low temperature and/or high growth rate may result in poor crystal quality. A more ideal solution would restrict the kinetics of island formation without sacrificing the kinetics of crystal growth.

A substantial modification of the growth mode is obtained by introducing a third element as a surfactant. If the surfactant lowers the surface free energy of both Ge and Si, segregation of the surfactant will be strongly favored during growth.

An atomistic point of view explains in more detail the way a surfactant changes the growth kinetics. We may assume that a Si or Ge atom has some mobility on the Sb monolayer, since we observe a smoothing of a rough intermediate phase.[26] Recent STM measurements also show a low number of defects in Ge films thicker than 12 ML,[5,21] even though they are rougher at lower coverages. On Si(001) a strongly localized exchange process was recently observed during As-mediated growth of Ge.[35] While a similar process may occur on the Si(111) Sb terminated surface, it would appear that 2D islanding and coarsening may be more important in this case, with exchange at steps playing a more prominent role. The steps may be intrinsic (due to sample miscut), or due to nucleation of two-dimensional islands on Si(111) terraces, depending on terrace size and surface diffusion length. During the Sb/Ge exchange, hardly any Sb is lost during the growth, even if no excess Sb is supplied. As soon as Ge or Si atoms occupy lattice sites underneath the Sb, their mobility is strongly hindered, due to the extra bonding to the Sb atoms. Islanding of the film caused by release of Ge or Si atoms from step or kink sites is now inhibited, without lowering the temperature or increasing the growth rate. Due to the high growth temperature, excellent crystal quality can be obtained.

The difference of the lattice constant of the elements A and B changes the situation in detail. Lattice strain-relieving defects are created for films exceeding a certain thickness. For Ge on Si(111) the first layers are grown pseudomorphically. In this starting phase the surface is somewhat rough, allowing some strain relief without creating dislocations, by elastic deformation toward the Ge lattice constant.[26,36,37]

As a thickness of 8 ML, defects are introduced, relieving the strain by the formation of dislocations. The growth front smoothens now,[26] since strain as a driving force for surface roughness is removed.

When a Ge film less than 8 ML thick is overgrown

with a 20-ML-thick Si cap, the LEED pattern shows a very smooth and highly perfect surface, even though the buried Ge/Se interface is rough. Thus, this intermediate roughness appears to be strain driven, relieving some of the lattice mismatch. The roughness observed on highly strained films is not the result of limited surface diffusion but of reduction of strain energy.[38] Si capping films grown on Ge films with thicknesses between 8 and 20 ML exhibit twinning, because the strain relieving defects in the Ge film (which in this thickness range come up to the surface) cannot be overgrown. In addition, Si films grown on top of (partially) relaxed Ge films are under tensile stress, causing the formation of strain-relieving defects in the Si cap.

V. SUMMARY

The experimental results presented above show that strain-relieved, low-defect Ge films may be grown on Si(111) with the use of an Sb monolayer adsorbed on the surface during growth. There are three different thickness regimes: below 8 ML, the Ge films are fully strained, exhibiting tetragonal distortion of the Ge lattice in order to accommodate to the Si lattice constant. Between 8 and roughly 20 ML, the Ge film contains defects, giving rise to a large increase in $\chi_{\min}$. These defects are present during the formation of an interfacial network of Shockley partial dislocations that eventually fully relieves the mismatch strain. Although the defects in this stage penetrate the film, threading to the surface, they disappear with increasing thickness. Thus, for thicknesses exceeding roughly 20 ML, the films have the Ge lattice constant and the threading portions of the defects have self-annihilated.

At no stage of growth do we observe large clusters when Sb is used. MEIS and Raman scattering see no evidence for Si-Ge intermixing, a common problem in Si-Ge growth. MEIS, TEM, and Raman scattering all show that the Ge films are of excellent crystal quality, with no more than 3×10^{19} Sb/cm^3 incorporated in the growing film, close to the solid solubility. In a separate paper we will show the temperature dependence of this Sb incorporation, with more incorporation and less perfect crystal quality at lower temperatures.[20]

Heteroepitaxial growth entails a delicate balancing between thermodynamical driving forces and kinetic limitations. With conventional growth techniques, temperature and growth rate are the only two variable parameters. This pitches film morphology against crystal quality, a dilemma with no satisfactory solution. Introduction of a third element during growth allows more freedom and a way out of the problem. We have shown that (near) saturation coverages of Sb on Si(111), and As or Sb on Si(001), eliminate islanding and interdiffusion. The adsorption of Ga on Si(111) also prevents islanding in heteroepitaxy, although domains of twinned orientation were found.[39] Furthermore, H was found effective at preventing interdiffusion during growth on Si(001).[40] This list is doubtlessly incomplete, because a limited number of studies have been reported; however, there is a high level of activity. In this paper we show that the presence of a surfactant may also have drastic effects on the defect structure of the epitaxial films. The change in strain-relief mechanisms under the presence of a surfactant was observed on both Si(001) and on Si(111). So far, Ge films grown on Si(001) remain defected at thicknesses exceeding 10 to 15 ML. However, the presence of a new type of strain-relief defect in these films points out the importance of the surfactant in determining the strain-relief mechanism.[8,9,41,42] It is likely that the change in film morphology induced by the surfactant layer is the most important factor in modifying the introduction of strain-relieving defects. A more direct mechanism, related to the presence of a surfactant monolayer, cannot be excluded, but is more elusive to study. We can only see the end result. Further studies of the defect generation mechanisms will be needed to make more progress in this area.

ACKNOWLEDGMENTS

We wish to thank Francoise LeGoues for many stimulating discussions. We thank Joe Demuth, and Sherrie Gillespie and Linda Ephrath (formerly with IBM Microelectronics Division, East Fishkill, NY) for their generous support and lively interest.

*Present address: Institut für Festkörperphysik, Universität Hannover, Appelstr. 2, 30167 Hannover, Germany.

[1]B. S. Meyerson, Sci. Am. **270**, 42 (1994).
[2]P. M. J. Marée, K. Nakagawa, F. M. Mulders, and J. F. van der Veen, Surf. Sci. **191**, 305 (1987).
[3]M. Copel, M. C. Reuter, E. Kaxiras, and R. M. Tromp, Phys. Rev. Lett. **63**, 632 (1989).
[4]M. Horn-von Hoegen, Appl. Phys. A (to be published).
[5]B. Voigtländer and A. Zinner, Appl. Phys. Lett. **63**, 3055 (1993).
[6]F. K. LeGoues, B. S. Meyerson, and J. F. Morar, Phys. Rev. Lett. **66**, 2903 (1991).
[7]E. A. Fitzgerald, Y. Xie, M. L. Green, D. Brasen, A. R. Korten, J. Michel, Y. Mii, and B. Weir, Appl. Phys. Lett. **59**, 811 (1991).
[8]M. Horn-von Hoegen, F. K. LeGoues, M. Copel, M. Reuter, and R. M. Tromp, Phys. Rev. Lett. **67**, 1130 (1991).
[9]F. K. LeGoues, M. Horn-von Hoegen, M. Copel, and R. M. Tromp, Phys. Rev. B **44**, 12 894 (1991).
[10]J. F. van der Veen, Surf. Sci. Rep. **5**, 199 (1985).
[11]R. M. Tromp, M. Copel, M. C. Reuter, M. Horn-von Hoegen, J. Speidell, and R. Koudis, Rev. Sci. Instrum. **62**, 2679 (1991).
[12]R. M. Tromp, H. H. Kersten, E. Granneman, F. W. Saris, R. J. Koudjis, and W. J. Kilsdonk, Nucl. Instrum. Methods B **46**, 155 (1984).
[13]J. C. Tsang, W. A. Thompson, and G. S. Oehrlein, J. Vac. Sci. Technol. B **3-4**, 1129 (1985).
[14]S. S. Iyer, J. C. Tsang, M. W. Copel, P. R. Pukite, and R. M. Tromp, Appl. Phys. Lett. **54**, 219 (1989).

[15]C. Park, T. Abukawa, T. Kinochita, Y. Enta, and S. Kono, Jpn. J. Appl. Phys. **27**, 147 (1988).
[16]P. Mårtensson, G. Meyer, N. M. Amer, E. Kaxiras, and K. C. Pandey, Phys. Rev. B **42**, 7230 (1990).
[17]T. Abukawa, C. Park, and S. Kono, Suf. Sci. **201**, L513 (1988).
[18]T. Kinoshita, Y. Enta, H. Ohta, Y. Yaegashi, S. Suzuki, and S. Kono, Surf. Sci. **204**, 405 (1988).
[19]G. Meyer (private communication).
[20]M. Horn-von Hoegen, J. Falta, M. Copel, and R. M. Tromp (unpublished).
[21]G. Meyer, B. Voigtlaender, and N. M. Amer, Surf. Sci. **274**, L541 (1992).
[22]K. Kajiyama, Y. Tanishiro, and K. Takayanagi, Surf. Sci. **222**, 38 (1989).
[23]K. Kajiyama, Y. Tanishiro, and K. Takayanagi, Surf. Sci. **222**, 47 (1989).
[24]T. Ichikawa and S. Ino, Surf. Sci. **136**, 267 (1983).
[25]M. Lamin, O. Pchelyakov, L. Sokolov, S. Stenin, and A. Toropov, Surf. Sci. **207**, 418 (1989).
[26]M. Horn-von Hoegen, M. Pook, A. Al Falou, B. H. Müller, and M. Henzler, Surf. Sci. **284**, 53 (1993).
[27]S. Mantl, E. Kasper, and H. Jorke, in *Heteroepitaxy on Silicon II*, edited by J. C. C. Fan, J. M. Phillips, and B.-Y. Tsaur, MRS Symposia Proceedings No. 91 (Materials Research Society, Pittsburgh, 1987), p. 305.
[28]T. Narusawa and W. M. Gibson, Phys. Rev. Lett. **47**, 1459 (1981).
[29]K. Fujita, S. Fukatsu, H. Yaguchi, T. Igarashi, Y. Shiraki, and R. Ito, Jpn. J. Appl. Phys. 2 **29**, L1981 (1990).
[30]K. Fujita, S. Fukatsu, Y. Shiraki, H. Yaguchi, and R. Ito, J. Crys. Growth **127**, 416 (1993).
[31]R. Metzger and F. Allen, J. Appl. Phys. **55**, 931 (1984).
[32]K. Nakagawa, M. Miyao, and Y. Shiraki, Jpn. J. Appl. Phys. **27**, L2013 (1988).
[33]W. Dondl, G. Lütjering, W. Wegscheider, J. Wilhelm, R. Schorer, and G. Abstreiter, J. Cryst. Growth **127**, 440 (1993).
[34]K. Sakamoto, K. Kyoyo, K. Miki, H. Matsuhata, and T. Sakamoto, Jpn. J. Appl. Phys. **32**, L204 (1993).
[35]R. M. Tromp and M. C. Reuter, Phys. Rev. Lett. **68**, 954 (1992).
[36]D. Eaglesham, H. Gossmann, and M. Cerullo, Phys. Rev. Lett. **65**, 1227 (1990).
[37]M. Horn-von Hoegen, B. H. Müller, and A. Al Falou (private communication).
[38]M. Horn-von Hoegen, A. Al Falou, B. H. Müller, U. Köhler, L. Andersohn, B. Dahlheimer, and M. Henzler, Phys. Rev. B **49**, 2637 (1994).
[39]J. Falta, M. Copel, F. K. LeGoues, and R. M. Tromp, Appl. Phys. Lett. **62**, 2962 (1993).
[40]M. Copel and R. M. Tromp, Appl. Phys. Lett. **58**, 2648 (1991).
[41]F. K. LeGoues, M. Copel, and R. M. Tromp, Phys. Rev. Lett. **63**, 1826 (1989).
[42]F. K. LeGoues, M. Copel, and R. M. Tromp, Phys. Rev. B **42**, 11 690 (1990).

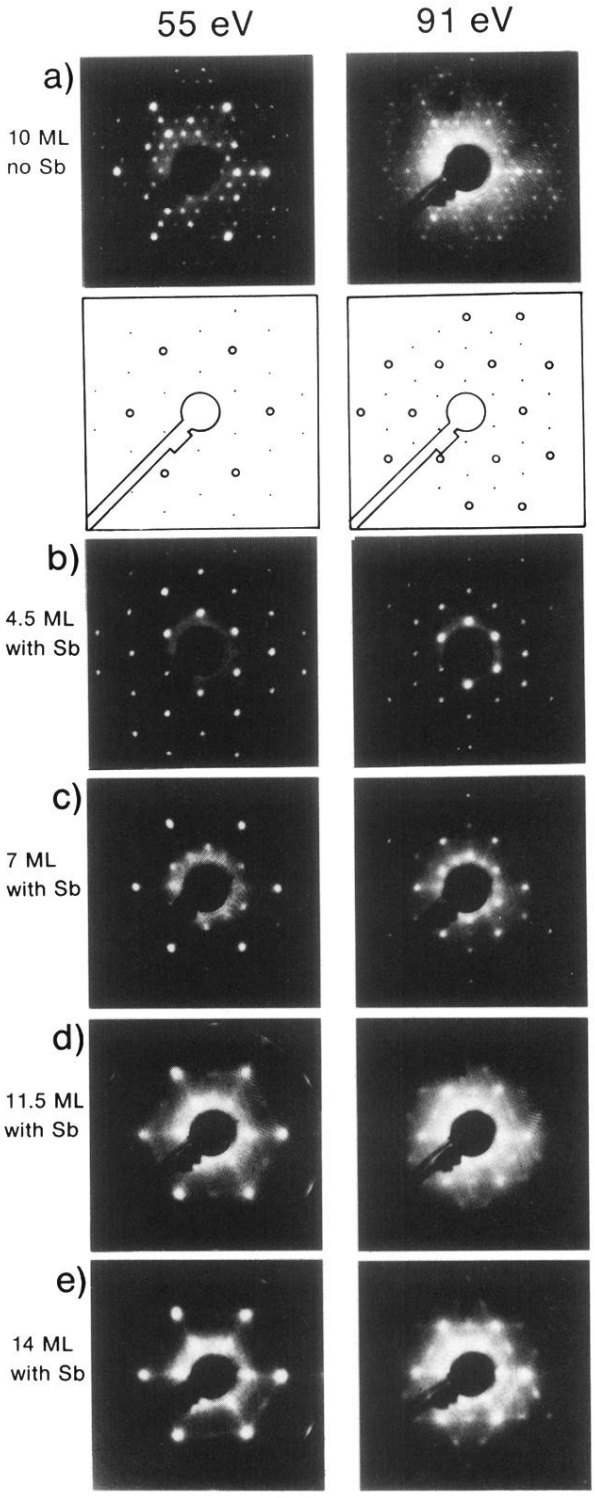

FIG. 3. LEED pattern of the films grown at 600 °C for electron energies of 55 and 91 eV. The inset shows the position of the integral order spots (circles) and the position of the $(\sqrt{3}\times\sqrt{3})$ spots (points). (a) 10 ML of Ge without surfactant results in a (5×5) reconstruction. (b)–(d) Different amounts of Ge covered with 20-ML Si grown with Sb as surfactant. The LEED pattern changes from a brilliant $(\sqrt{3}\times\sqrt{3})$ reconstruction with low background (4.5-ML Ge) to a mixture of diffuse (2×1) and $(\sqrt{3}\times\sqrt{3})$ reconstruction with high background (14-ML Ge), indicating increasing defect densities.

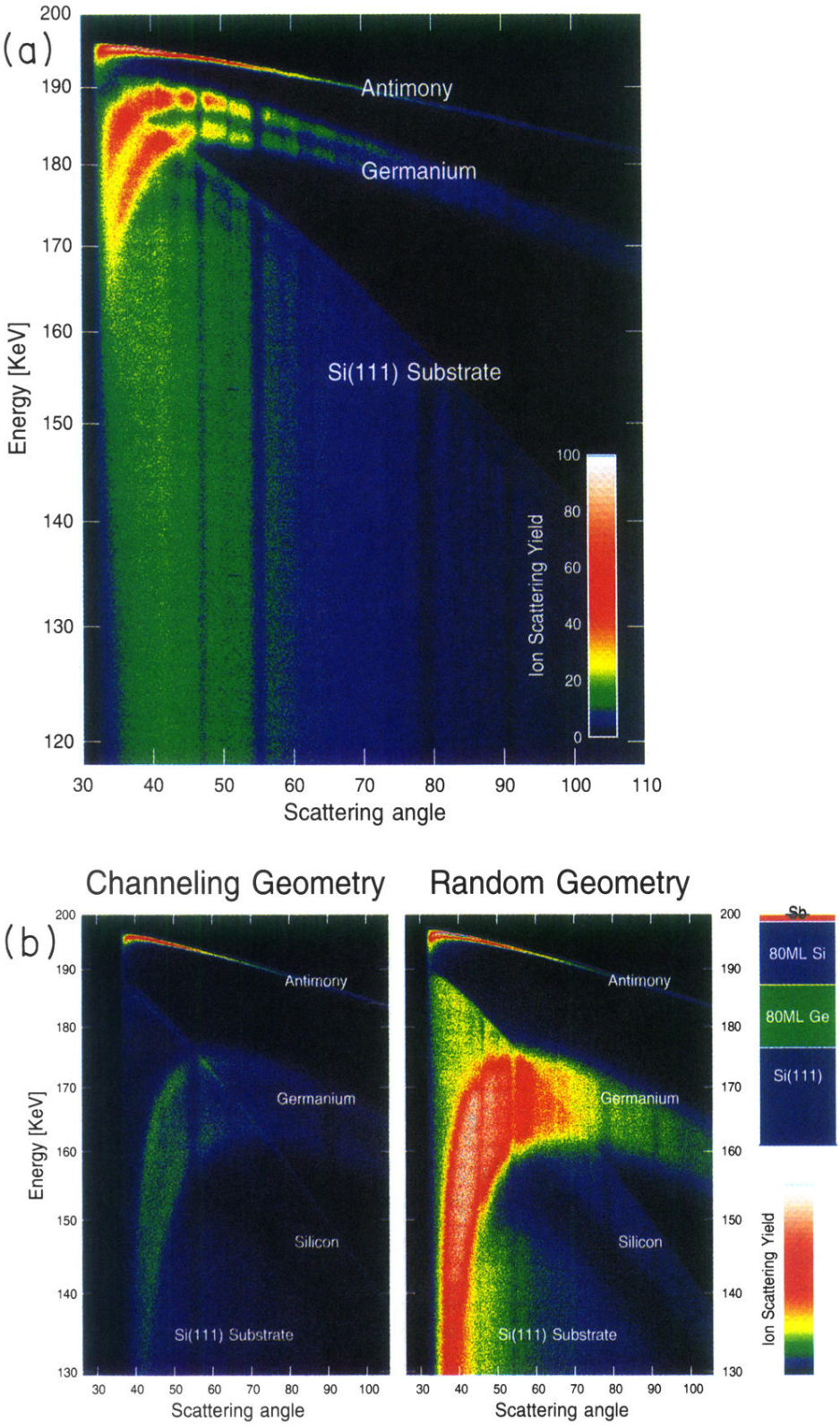

FIG. 7. Ion backscatter spectra for different Ge/Si layered structures are shown. He^+ ions with 200 keV have been used. The yield is plotted using the color look-up table shown in the inset. The ion backscatter yield is plotted both as a function of the scattering angle (x axis) and of the backscattered ion energy (y axis). (a) A Si(111)/Ge_5/Si_{10}/Ge_5/Si_{15}/Sb layered structure (the subscripts indicate the thickness of the particular layer in ML) grown at 600 °C. The depth location of the two Ge layers is apparent in the weak dips in the Si signal. (b) A relaxed 80-ML Si film grown on top of a 80-ML Ge film on Si(111). Both random and channeling spectra are shown. The Ge has been deposited at 600 °C substrate temperature which has been raised up to 700 °C for the growth of the Si layer. The Sb adlayer is the topmost fine sharp line. The blocking minima are seen as vertical lines with lower intensity. The embedded Ge film is seen as an intense broadband. In the channeling spectra the location of the strain-relieving dislocations is clearly seen in the increased yield at the borders of the Ge signal.